J. Fluid Mech. (1996), vol. 326, pp. 399–415

Three-dimensional instability of axisymmetric buoyant convection in cylinders heated from below

By M. WANSCHURA, H. C. KUHLMANN AND H. J. RATH

Center of Applied Space Technology and Microgravity, ZARM - University of Bremen, Am Fallturm, 28359 Bremen, Germany

(Received 15 November 1995 and in revised form 11 June 1996)

The stability of steady axisymmetric convection in cylinders heated from below and insulated laterally is investigated numerically using a mixed finite-difference/Chebyshev collocation method to solve the base flow and the linear stability equations. Linear stability boundaries are given for radius to height ratios Γ from 0.9 to 1.56 and for Prandtl numbers $Pr = 0.02$ and $Pr = 1$. Depending on Γ and Pr, the azimuthal wavenumber of the critical mode may be $m = 1, 2, 3$, or 4. The dependence of the critical Rayleigh number on the aspect ratio and the instability mechanisms are explained by analysing the energy transfer to the critical modes for selected cases. In addition to these results the onset of buoyant convection in liquid bridges with stress-free conditions on the cylindrical surface is considered. For insulating thermal boundary conditions, the onset of convection is never axisymmetric and the critical azimuthal wavenumber increases monotonically with Γ. The critical Rayleigh number is less then 1708 for most aspect ratios.

1. Introduction

A liquid layer heated from below and cooled from above is a basic problem in geophysics and in many heat transfer problems in technical applications. For that reason Rayleigh–Bénard convection is one of the most intensively studied hydrodynamical systems. Besides its practical importance it also serves as the most important pattern-forming dynamical system in continuous dissipative media, since the symmetry of the flow is successively broken when the temperature difference is increased, leading to a wealth of different spatio-temporal patterns (see e.g. Koschmieder 1993).

Here we will be concerned with the Rayleigh–Bénard problem in a finite volume bounded laterally by a cylindrical surface on which different boundary conditions for the velocity field may be imposed. In particular, we will focus on the secondary transition from steady two-dimensional axisymmetric flows to three-dimensional convection patterns.

Compared to the buoyant flow between parallel plates of infinite extent (Busse 1978) the cylindrical problem has received less attention, partly due to the complications introduced by the lateral boundaries. The primary instability of the motionless heat conductive state in the latter system has been well established since the work of Charlson & Sani (1970, 1971), Stork & Müller (1975), Rosenblat (1982), and Buell & Catton (1983). The critical Rayleigh number for the first onset of steady

convection is independent of the Prandtl number. The azimuthal wavenumber m of the critical mode depends on the aspect ratio $\Gamma = R/d$ (R is radius, d is height) and approaches the value $Ra_{c1} = 1708$ asymptotically for $\Gamma \to \infty$. Secondary instabilities, however, have only been explored for a few exceptional cases. The reason is that even the primary flow from which the secondary flow bifurcates is typically three-dimensional from the onset of convection. Any further numerical analyses thus require full three-dimensional calculations (see e.g. Crespo del Arco & Bontoux 1989). Exceptions are finite ranges of the aspect ratio for which the primary instability is axisymmetric ($m = 0$). High-accuracy numerical calculations of the linear stability of these axisymmetric buoyant flows are possible due to normal mode decomposition of the azimuthal dependence of the neutral mode. Our investigation will focus on the linear stability of these axisymmetric flows in the range $0.9 < \Gamma < 1.57$.

The first numerical investigation of the stability of steady axisymmetric flows is due to Charlson & Sani (1975). They used a Galerkin method to calculate the basic flows, the linear stability of which was then analysed by expanding the disturbances into the same set of basis functions as were used for the base states. The analysis, however, failed in satisfactorily predicting the secondary instability, since the mode truncation was too severe.

Müller, Neumann & Weber (1984) investigated the flow patterns both numerically and experimentally for $Pr = 0.02$ (liquid metals) and $Pr = 6.7$ (water). Experimentally, they found for both Prandtl numbers that the axisymmetric base flows are quite stable for $\Gamma = 1$. For $Pr = 6.7$, for example, the base flow ($m = 0$) was found to be stable up to $\approx 10Ra_{c1}$ in qualitative agreement with their numerical simulation. A second stable solution was found numerically to exist at $Ra = 2800$ with symmetry $m = 2$. This result was also reported by Neumann (1990). A corresponding three-dimensional flow, however, was not observed in the experiment.

Hardin & Sani (1993) investigated the amplitude and the stability properties of the primary solution using a slightly nonlinear approximation by retaining only the six most significant modes of an expansion in terms of the eigenfunctions of the linear stability problem of the conducting state. Even though they expected their approach "to appear more likely to suggest potential secondary bifurcations" they identified a secondary bifurcation at $Ra_{c2} = 2850$ for $\Gamma = 1$ and $Pr = 6.7$ at which the axisymmetric solution becomes unstable to a stable mode with $m = 2$. The instability of the axisymmetric flow is in contradiction to the results of Müller *et al.* (1984) and Neumann (1990). A similar branching from axisymmetric flow to an $m = 2$ mode was found at $Ra_{c2} = 2430$ for $\Gamma = 1$ and $Pr = 0.02$. Note that these values of the second critical Rayleigh number Ra_{c2} are close to the neutral value for the instability of the conducting state with respect to the mode $m = 2$, which is $Ra_{c1}(\Gamma = 1, m = 2) = 2493$ (Hardin & Sani 1993).

Recently, Wagner, Friedrich & Narayanan (1994) numerically simulated the flow for $\Gamma = 1$ using similar initial conditions as Neumann (1990). They showed for $Pr = 6.7$ and $Ra = 2800$ that the decay rate of an initial disturbance with symmetry $m = 2$ is significantly influenced by the grid resolution. For a sufficient number of grid points the $m = 2$ flow at $Ra = 2800$ decays to a pure axisymmetric flow in contradiction to Neumann (1990) and to the numerical result of Müller *et al.* (1984).

To date, the numerical data for the secondary buoyant instability in cylinders do not cover all aspect ratios and Prandtl numbers. Even for $\Gamma = 1$ and $Pr = 6.7$ no reliable critical values for the instability of the axisymmetric flows are available.

This work is mainly aimed at calculating the linear stability boundaries of the buoyant axisymmetric basic flow in rigid cylinders for aspect ratios $0.9 < \Gamma < 1.57$.

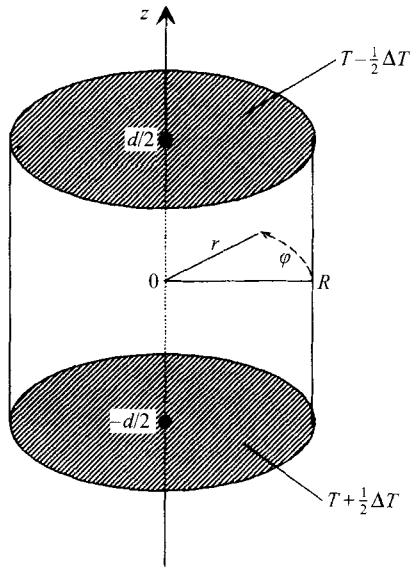

FIGURE 1. Geometry and coordinate system.

The linear two-dimensional equations governing the evolution of three-dimensional disturbances of a given azimuthal wavenumber can be solved much more accurately to yield the second critical Rayleigh number Ra_{c2} than would be possible within a three-dimensional numerical simulation or a weakly nonlinear theory. Moreover, the above aspect ratio range can be covered quasi-continuously. An *a posteriori* energy analysis is employed to explain the physics of the secondary instabilities. Apart from contributing to the analysis of the bifurcation sequence of Rayleigh–Bénard convection in cylinders this investigation should also contribute to a better understanding of the transitions observed in experiments, where sidewall forcing may obscure the ideal patterns.

2. Statement of the problem

We consider a liquid volume bounded by a cylindrical container of radius R and height d (figure 1) which is heated from below by keeping the top and the bottom of the cylinder at constant temperatures $T_0 - \Delta T/2$ and $T_0 + \Delta T/2$, respectively. T_0 is the mean temperature and the aspect ratio is defined as $\Gamma = R/d$. Using the scales d, ν/d, $\rho_0 \nu^2/d^2$, ΔT and d^2/ν for length, velocity, pressure, temperature, and time, where ν and ρ_0 denote the kinematic viscosity and density, the transport equations for momentum and heat in the Boussinesq approximation are

$$(\partial_t + \boldsymbol{U} \cdot \nabla)\, \boldsymbol{U} = -\nabla P + \Delta \boldsymbol{U} + \frac{Ra}{Pr} \Theta \boldsymbol{e}_z, \tag{2.1}$$

$$(\partial_t + \boldsymbol{U} \cdot \nabla)\, \Theta = W + \frac{1}{Pr} \Delta \Theta, \tag{2.2}$$

$$\nabla \cdot \boldsymbol{U} = 0, \tag{2.3}$$

where $\boldsymbol{U} = (U, V, W)$, P, and Θ denote the dimensionless velocity, pressure, and temperature fields. Θ is the deviation from the linear conducting profile

$$T = T_0 + \Delta T(\Theta + \Theta_{cond}); \quad \Theta_{cond} = -z. \tag{2.4}$$

The dimensionless parameters arising are the Prandtl and Rayleigh numbers, defined as

$$Pr = \frac{\nu}{\kappa},$$

$$Ra = \frac{\alpha \Delta T g \, d^3}{\kappa \nu},$$

where κ is the thermal diffusivity, g the acceleration due to gravity, and α the thermal expansion coefficient at constant pressure

$$\alpha = -\frac{1}{\rho_0}\left(\frac{\partial \rho}{\partial T}\right)_p. \tag{2.5}$$

The no-slip, no-penetration, and constant-temperature boundary conditions at the top and bottom walls ($z = \pm\frac{1}{2}$) are

$$\boldsymbol{U} = \Theta = 0. \tag{2.6}$$

On the circumference of the cylinder we impose no penetration and thermal insulation,

$$U = \partial_r \Theta = 0, \tag{2.7}$$

together with boundary conditions for the tangential velocities. These will be either no-slip

$$V = W = 0, \tag{2.8}$$

or free-slip conditions

$$\left(\partial_r - \frac{1}{r}\right) V = \partial_r W = 0. \tag{2.9}$$

The free slip conditions apply to a liquid bridge with a non-deformable free surface in the absence of the Marangoni effect and other surface forces. Proper symmetry conditions on the axis complete the problem.

3. Numerical solution techniques

The numerical methods used are the same as applied previously to thermocapillary flow instabilities in cylindrical liquid bridges. For details of the schemes, including the validation of the codes, the reader is referred to Wanschura *et al.* (1995).

3.1. *Basic state*

To calculate the steady axisymmetric flow ($V = \partial_\varphi = \partial_t = 0$), we use a stream function–vorticity–formulation of (2.1)–(2.3). The resulting system of differential equations is approximated by a set of algebraic equations obtained by application of a Chebyshev collocation method in the radial direction and a second-order finite-difference scheme in the axial direction. The discretized equations, including the boundary conditions, are linearized and solved implicitly by Newton–Raphson iteration.

3.2. *Linear stability analysis*

The stability of the non-trivial two-dimensional axisymmetric solution $(\boldsymbol{U}, P, \Theta)$ as well as that of the conducting motionless state is investigated with linear stability theory. Linearizing (2.1)–(2.3) with respect to small perturbations $(\boldsymbol{u}, p, \theta)$ of the base

state yields

$$\partial_t \boldsymbol{u} + (\boldsymbol{u}\cdot\nabla)\,\boldsymbol{U} + (\boldsymbol{U}\cdot\nabla)\,\boldsymbol{u} = -\nabla p + \Delta\boldsymbol{u} + \frac{Ra}{Pr}\theta\boldsymbol{e}_z, \tag{3.1}$$

$$\partial_t\theta + (\boldsymbol{u}\cdot\nabla)\,\Theta + (\boldsymbol{U}\cdot\nabla)\,\theta = w + \frac{1}{Pr}\Delta\theta, \tag{3.2}$$

$$\nabla\cdot\boldsymbol{u} = 0. \tag{3.3}$$

The general solution of this linear system of equations is a superposition of normal modes

$$\begin{pmatrix} \boldsymbol{u} \\ p \\ \theta \end{pmatrix} = \mathrm{e}^{\tilde{\alpha}t}\,\mathrm{e}^{\mathrm{i}m\varphi}\begin{pmatrix} \boldsymbol{u}(r,z) \\ p(r,z) \\ \theta(r,z) \end{pmatrix} + \text{c.c.}, \tag{3.4}$$

where m is an integer azimuthal wavenumber and $\tilde{\alpha} = \alpha + \mathrm{i}\omega$ with growth rate α and oscillation frequency ω. Inserting (3.4) and using the same discretization as for the basic state, we obtain a generalized eigenvalue problem

$$\boldsymbol{A}\boldsymbol{x} = \tilde{\alpha}\boldsymbol{B}\boldsymbol{x}, \tag{3.5}$$

where $\tilde{\alpha}$ is the eigenvalue and $\boldsymbol{x}$ denotes the eigenvector of field entities. $\boldsymbol{A}$ and $\boldsymbol{B}$ are the matrix representations of the set of linear volume equations and boundary conditions.

A treatment of the volume equations (3.1)–(3.3) requires the distinction between $m = 0$ and $m > 0$. For $m = 0$ we use a stream function–vorticity formulation similar to the basic-state calculation. For $m > 0$ the azimuthal velocity v is eliminated using the continuity equation and the eigenvalue problem (3.5) is formulated in terms of the primitive variables (u, w, p, θ). It is solved by inverse iteration. The stability limits are found by a zero search with respect to the real part α of the eigenvalue corresponding to the most dangerous mode.

3.3. *Energy analysis*

To investigate the physical mechanisms leading to the instability, we analyse the energy transfer between the basic state and the critical mode. The rate of change of the (non-dimensional) kinetic energy E_{kin} is given by the Reynolds–Orr equation obtained by multiplying (3.1) with $\boldsymbol{u}$ and integrating over the volume $\mathscr{V}$ occupied by the fluid. Similarly, a balance for the 'thermal energy' E_T, i.e. a positive measure of the neutral temperature field, is obtained by multiplying (3.2) with θ followed by a volume integration. Taking into account the boundary conditions and using Green's theorem, the rate of change of the kinetic and thermal energies can be written as

$$\frac{\mathrm{d}E_{kin}}{\mathrm{d}t} = \frac{1}{2}\frac{\mathrm{d}}{\mathrm{d}t}\int_{\mathscr{V}} \boldsymbol{u}^2\mathrm{d}^3r = -D + I_v + \frac{Ra}{Pr}I_{T3}, \tag{3.6}$$

$$\frac{\mathrm{d}E_T}{\mathrm{d}t} = \frac{1}{2}\frac{\mathrm{d}}{\mathrm{d}t}\int_{\mathscr{V}} \theta^2\mathrm{d}^3r = -D_T + I_T. \tag{3.7}$$

D and D_T are the rates of viscous dissipation and heat diffusion, respectively,

$$D = \int_{\mathscr{V}} (\nabla\times\boldsymbol{u})^2\mathrm{d}^3r - 2\int_{\mathscr{S}}\left(\frac{v^2}{r}\right)_{r=\Gamma}\mathrm{d}^2r, \qquad D_T = \frac{1}{Pr}\int_{\mathscr{V}}(\nabla\theta)^2\mathrm{d}^3r, \tag{3.8}$$

where $\mathscr{S}$ is the radial surface of the volume. I_v denotes integrals resulting from the interaction between the disturbance $\boldsymbol{u}$ and the basic flow $\boldsymbol{U}$:

$$I_v = I_{v1} + I_{v2} + I_{v3} + I_{v4} + I_{v5}$$
$$= -\int_{\mathscr{V}} \left[U\frac{v^2}{r} + u^2\frac{\partial U}{\partial r} + uw\frac{\partial U}{\partial z} + wu\frac{\partial W}{\partial r} + w^2\frac{\partial W}{\partial z} \right] \mathrm{d}^3 r, \tag{3.9}$$

and I_T arises due to convective transport of thermal energy of the basic temperature field $\Theta + \Theta_{cond}$:

$$I_T = I_{T1} + I_{T2} + I_{T3} = -\int_{\mathscr{V}} \theta \left(u\frac{\partial \Theta}{\partial r} + w\frac{\partial \Theta}{\partial z} - w \right) \mathrm{d}^3 r. \tag{3.10}$$

For unstable basic states ($\alpha > 0$) and three-dimensional disturbances ($m > 0$), it can easily be shown analytically that the rate of change of kinetic and thermal energy is always positive ($\partial_t E_{kin} > 0, \partial_t E_T > 0$). This also holds for oscillating modes because all oscillatory terms in the energy balances vanish after the volume integration. Therefore, terms on the right-hand side of (3.6) and (3.7) with a positive (negative) sign are destabilizing (stabilizing) the base flow. Since D and D_T are positive, they are stabilizing. However, the sign and the magnitude of I_v and I_T depends sensitively on both the neutral mode and the basic state.

The energy change rates are calculated on an interpolated equidistant grid using a second-order finite-difference scheme. Integrations are carried out using Simpson's rule. Since the energy equations (3.6) and (3.7) must be exactly satisfied by any solution of the linear stability problem, we define the relative error in the kinetic energy balance as the residual normalized by the largest absolute value of the integrals on the right-hand side of (3.6):

$$\delta_{kin} := \frac{|-\partial_t E_{kin} - D + I_v + I_{Gr}|}{\max\{D, |I_{v1}| \ldots |I_{v5}|, |I_{Gr}|\}},$$

where $I_{Gr} = (Ra/Pr)I_{T3}$. The error for the thermal energy balance δ_T is defined accordingly:

$$\delta_T := \frac{|-\partial_t E_T - D_T + I_T|}{\max\{D_T, |I_{T1}|, |I_{T2}|, |I_{T3}|\}}.$$

4. Results

Various convergence tests were performed to assure sufficient numerical accuracy. All stability limits presented here are well converged on a grid of 16 radial collocation points and 100 axial finite-difference steps. Energy errors were in no case larger than $\delta_{kin} = 2\%$ and $\delta_T = 1\%$, respectively.

4.1. *Instability of the state of rest*

As a first step, the instability of the conducting state was calculated, both to compare the critical Rayleigh numbers with those given in the literature and to determine the Γ-region where $m = 0$ is the critical mode.

Figure 2 shows the stability diagram for the conductive basic state using no-slip conditions at $r = \Gamma$. The critical Rayleigh number for the onset of stationary convection is plotted versus the aspect ratio for modes with azimuthal wavenumbers $m = 0, 1$, and 2. In the region shown, the critical mode is axisymmetric ($m = 0$) within two Γ-intervals. These results are in excellent agreement with those of Hardin *et al.*

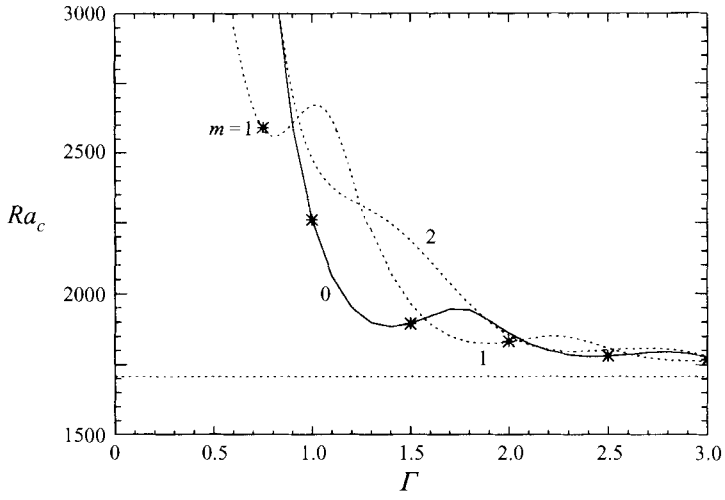

FIGURE 2. Curves of neutral stability for the onset of convection with no-slip conditions imposed on the cylinder circumference. The horizontal dotted line marks $Ra_{c1}^{\Gamma=\infty} = 1708$. Asterisks: Comparison with linear stability results of Hardin *et al.* (1990).

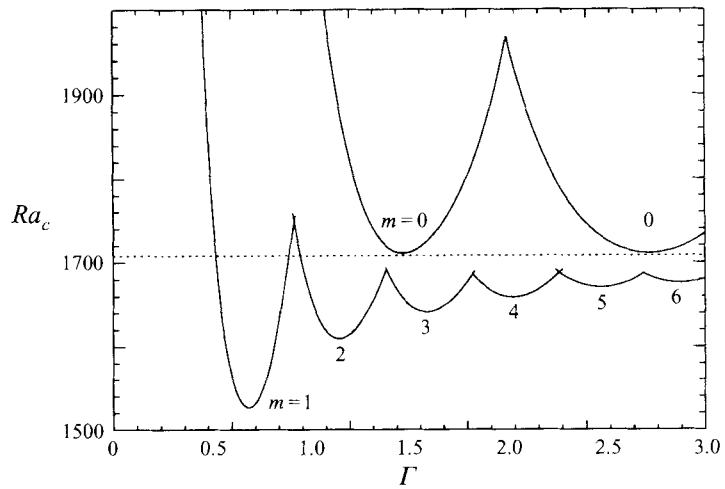

FIGURE 3. Curves of neutral stability for the onset of convection with free-slip conditions imposed on the cylinder circumference. The horizontal dotted line marks $Ra_{c1}^{\Gamma=\infty} = 1708$.

(1990) (asterisks in figure 2). The critical Rayleigh number approaches the limit for an infinite layer $Ra_{c1}^{\infty} = 1708$ with increasing Γ (dotted line). More details on the asymptotic behaviour can be found in Chen (1992*a*, *b*).

Apart from rigid boundary conditions, artificial 'slip' boundary conditions $(\partial_r + 1/r)v = 0$, $\partial_r w = 0$ on the surface at $r = \Gamma$ have also been employed previously by Rosenblat (1982) and Chen (1992*a*, *b*). This boundary condition, which expresses the vanishing of the vertical vorticity at $r = \Gamma$, allows a separation of variables for the neutral mode. In contrast, the free-slip (zero-stress) condition requires $(\partial_r - 1/r)v = 0$ at $r = \Gamma$. Both boundary conditions are identical only for axisymmetric modes ($m = 0$), in which case $v \equiv 0$. The free-slip condition on $r = \Gamma$ has not been considered to date. This condition, however, is relevant to convection in *liquid bridges*

m	0	0	1	2	3	4	5	6
Γ	1.22	2.26	0.57	0.95	1.32	1.69	2.06	2.39
Ra_{c1}	1711	1711	1527	1609	1642	1659	1670	1676

TABLE 1. Minimum critical Rayleigh numbers Ra_{c1} with respect to Γ for different m for the instability of the conducting state with *free-slip* boundary conditions.

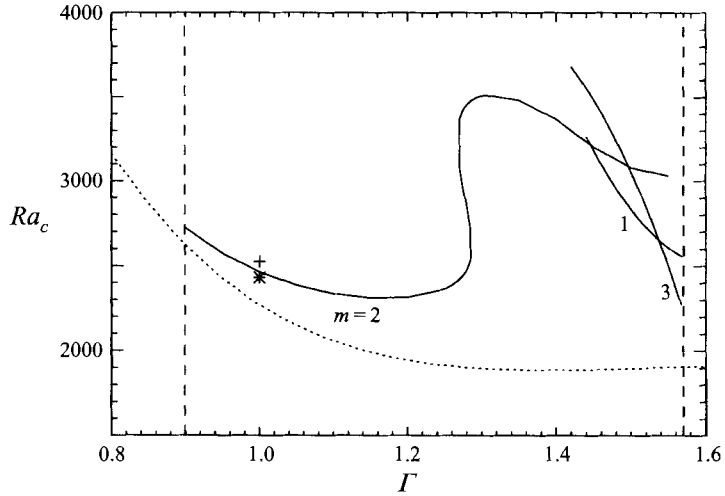

FIGURE 4. Neutral stability curves for the three-dimensional instability of the axisymmetric basic flow in the interval $0.9 < \Gamma < 1.57$ for $Pr = 0.02$. The dotted line marks the onset of two-dimensional convection. Cross: Neumann (1990), asterisk: Hardin & Sani (1993).

(Wanschura *et al.* 1995) modelling the floating-zone crystal growth process (Bohm, Lüdge & Schröder 1994). In the limit of large surface tension, a liquid bridge of appropriate volume takes a perfectly cylindrical shape. We find that for such liquid bridges with stress-free surfaces, the onset of convection is never axisymmetric (at least for $\Gamma < 2.5$) if Marangoni effects are absent. The corresponding stability diagram is shown in figure 3. The minimum values for Ra_{c1} for different m are given in table 1. It is interesting to note that the asymptotic value $Ra_{c1}^{\infty} = 1708$ is approached from below in this case. The strict order with respect to m (at least up to $m = 6$) of the different instability domains is remarkable. In agreement with our results for $m = 0$, Chen (1992*b*) and Rosenblat (1982) have shown that the minima of the critical curves touch the line $Ra = Ra_{c1}^{\infty}$, if zero vertical vorticity is imposed at $r = \Gamma$.

In the following, we will focus on rigid boundary conditions and aspect ratios in the interval $0.9 < \Gamma < 1.57$, where the first instability is axisymmetric. We calculate the supercritical convective nonlinear axisymmetric basic solutions for this case and analyse their stability with respect to three-dimensional disturbances mainly for two representative Prandtl numbers, namely $Pr = 0.02$ (liquid metals) and $Pr = 1$ (transparent liquids).

4.2. *Instability of steady axisymmetric convection*

4.2.1. $Pr = 0.02$

Figure 4 shows the stability diagram for the second instability at $Pr = 0.02$. Some numerical values are given in table 2 (including values for $Pr = 1$). In

	$Pr = 0.02$		$Pr = 1$		
Γ	Ra_{c2}	m	Ra_{c2}	m	ω_{c2}
0.9	2721	2	2619	1	0
0.95	2572	2	2961	2	0
1.0	2463	2	3017	2	0
1.0896			3911	2	0
1.1	2336	2	8321	1	0
1.2	2315	2	12821	1	0
1.275	2443	2			
1.275	3423	2			
1.3	3506	2	17552	1	0
1.35	3480	2			
1.4	3368	2	22493	1	0
1.45	3174	1			
1.47			24928	3	$\pm$42.54
1.5	2831	1	24536	3	$\pm$42.26
1.57	2234	3	23011	4	$\pm$45.47

TABLE 2. Critical Rayleigh numbers Ra_{c2} for the onset of three-dimensional convection.

the investigated Γ-interval, the axisymmetric basic flow becomes unstable to three-dimensional stationary ($\omega = 0$) disturbances with azimuthal wavenumbers $m = 1, 2,$ and 3. The basic solution is not unique: two solutions exist that can be transformed one into the other by $(z, U, W, \Theta) \rightarrow (-z, U, -W, -\Theta)$ (Liang, Vidal & Acrivos 1969). The same symmetry applies to the disturbances. Thus the critical Rayleigh numbers are the same for both solutions.

Our results are in good agreement with previous calculations. Neumann (1990) performed a three-dimensional time-dependent simulation of the present problem and found the onset of three-dimensional convection with azimuthal symmetry $m = 2$ for $Pr = 0.02$ and $\Gamma = 1$ at $Ra_{c2} = 2525$. This value is 2.5% larger than our value of $Ra_{c2} = 2463$. Hardin & Sani (1993) found $Ra_{c2} = 2430$ for this case using a weakly nonlinear approach. This value is 1.3% less than ours.

In the Γ-interval where $m = 2$ is the critical wavenumber, the strong increase of the critical Rayleigh number at $\Gamma = 1.275$ is remarkable. For small Pr the thermal energy is just a balance between heat conduction (D_T) and I_{T3}. It is unimportant for the instability mechanism. The kinetic energy balance for $\Gamma = 1.275$ is shown in figure 5. The basic solution becomes unstable first at $Ra = 2443$. For $Ra > 2443$, I_{v3} is growing, being responsible for the instability. However, the decrease of the work done by buoyant forces I_{Gr} relative to the dissipation and the stabilization due to I_{v4} leads to a linearly stable window $2957 < Ra < 3423$. For higher Ra, the basic flow becomes unstable again. Within this second domain of instability, I_{v3} seems to saturate, whereas the stabilization due to I_{v4} gets much weaker (I_{v4} grows). Nevertheless, I_{v3} and I_{Gr} remain the sources of energy. The particular shape of the stability boundary is thus due to a change of the instability mechanism. For $\Gamma \lesssim 1.275$ the most destabilizing terms are I_{v3} and I_{Gr}, while for $\Gamma \gtrsim 1.275$ I_{v4} becomes positive and contributes to the energy growth, eventually becoming the most destabilizing term.

I_{v3} is a measure for the amplification of radial velocity disturbances (u) by axial transport (w) of axial gradients of the basic radial flow ($\partial_z U$). Similarly, I_{v4} describes the amplification of axial velocity disturbances (w) by radial transport (u) of axial

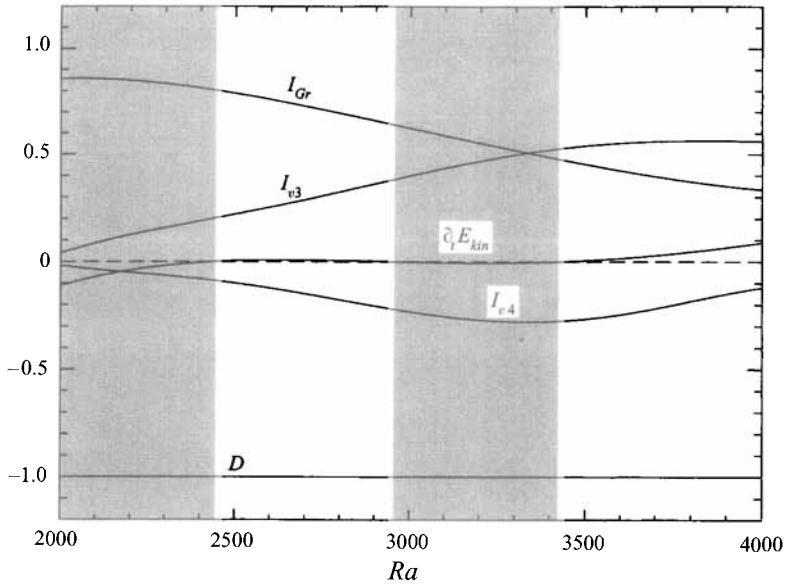

FIGURE 5. The rate of change of kinetic energy as a function of Ra for $\Gamma = 1.275$, $Pr = 0.02$, $m = 2$. All terms are normalized with respect to D. Shaded areas indicate linear stability.

shear ($\partial_r W$) (cf. (3.9)). These amplifications lead to instability due to a feedback mechanism based on continuity and the finite volume of the cylinder (see also Wanschura *et al.* 1995). Even though the conventional buoyancy term $I_{Gr} = (Ra/Pr)I_{T3}$ contributes to the energy growth at low Pr, its relative importance diminishes for increasing Ra.

It can be shown that the change of the instability mechanism is related to a radial outward shift of the basic-state vortex for increasing Γ. Owing to this shift, a region of vertical shear appears near the axis ($r = 0$) from which the neutral mode extracts its energy via I_{v4}. This has been proved by considering the space dependence (not shown) of the integrand of I_{v4}.

While the destabilizing action of I_{v4} increases, I_{v3} becomes less important when Γ is increased. Owing to the displacement of the basic vortex, the radial shear ($\partial_z U$) entering I_{v3} arises in a smaller fraction of the cylinder volume. In addition to that, more stabilizing contributions to the integral I_{v3} (not shown) appear with increasing Γ, which are caused by structural changes of the critical mode.

In the region where $m = 1$ and $m = 3$ are the critical modes (figure 4), I_{v4} is still the most destabilizing term and the above-discussed mechanism equally holds.

4.2.2. $Pr = 1$

Figure 6 shows the stability diagram for for $Pr = 1$. The dependence of the critical wavenumber and the critical Rayleigh number on Γ is different from $Pr = 0.02$ (figure 4). The solid curves for $m = 1, 2$ indicate stationary instabilities, while the dashed ones for $m = 3, 4$ represent oscillatory Hopf bifurcations. For $Pr = 1$, $m = 1$ is critical in a wide interval, whereas for $Pr = 0.02$, $m = 2$ is the dominating critical wavenumber. A distinguished feature is the turning of the neutral curve for $m = 2$. There exists a linearly stable region of Rayleigh numbers for $\Gamma \approx 1.05 - 1.09$ within which either a decrease or an increase of Ra will cause three-dimensional convection.

The three-dimensional time-dependent simulation of Neumann (1986) predicts

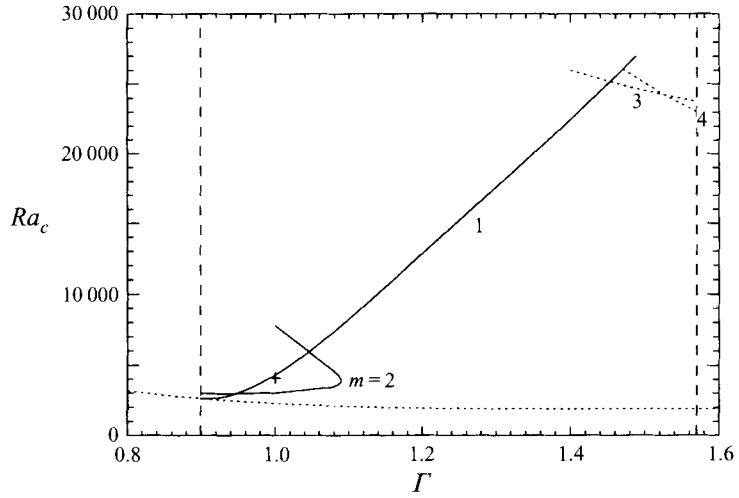

FIGURE 6. Neutral stability curves for the three-dimensional instability of the axisymmetric basic flow in the interval $0.9 < \Gamma < 1.57$ for $Pr = 1$. The lower dotted line marks the onset of two-dimensional convection. The instabilities for $m = 3$ and $m = 4$ are oscillatory. Cross: Neumann (1986).

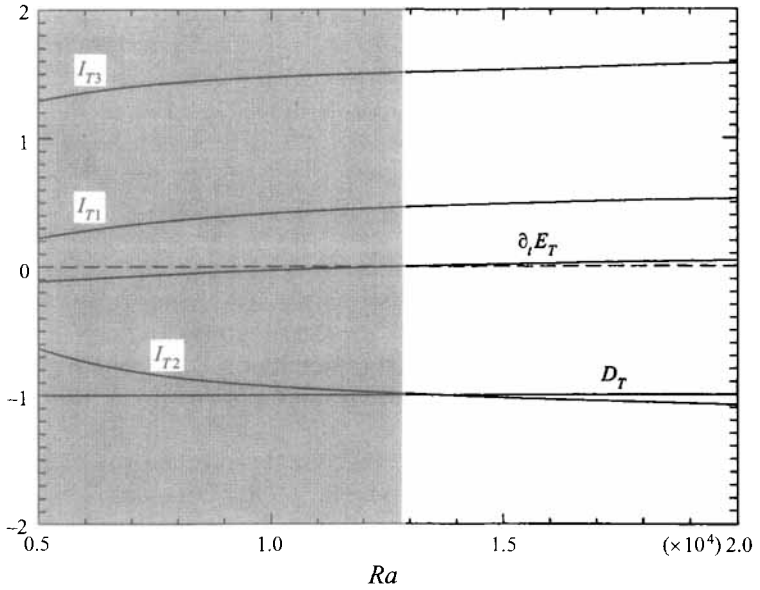

FIGURE 7. The rate of change of thermal energy as a function of Ra for $\Gamma = 1.2$, $Pr = 1$, $m = 1$. All terms are normalized with respect to D_T. The shaded area indicates linear stability.

three-dimensional convection with $m = 1$ symmetry for $Pr = \Gamma = 1$ and $Ra > 4100$. This value is only 2.9% smaller than our neutral value ($Ra_{c2}^{m=1} = 4224$). However, the critical limit for $m = 2$ is smaller ($Ra_{c2}^{m=2} = 3016$).

Figure 7 shows the thermal energy balance as a function of Ra for $\Gamma = 1.2$ and $m = 1$. The kinetic balance shows no dependence of the different terms on Ra and is therefore not important for the instability mechanism. The most destabilizing contribution with respect to an increase of Ra is $I_{T3} = \int_V \theta w \mathrm{d}^3 r$. It is a measure of

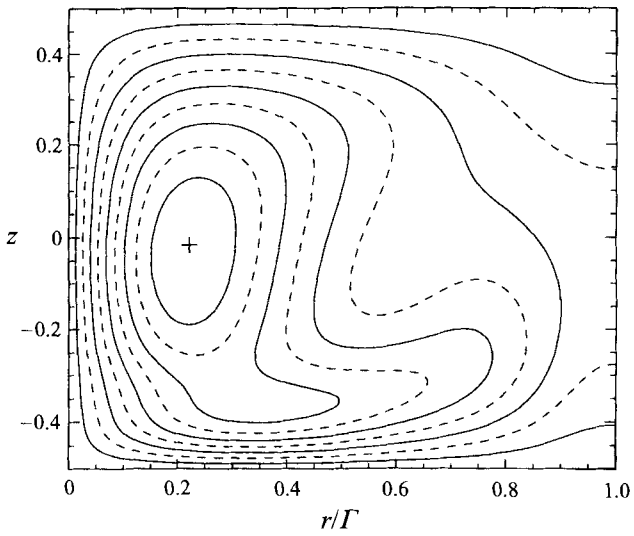

FIGURE 8. Temperature field of the critical mode at $\varphi = 0$ for $\Gamma = 1.2$, $Pr = 1$, $Ra_{c2} = 12821$, $m = 1$.

the amplification of temperature disturbances (θ) due to the axial transport (w) of axial gradients of the conductive linear temperature profile ($\partial_z \Theta_{cond} = -1$). This is the classical buoyancy term.

Note that even though this mechanism is the conventional thermal instability, the onset Rayleigh number is $Ra_{c2} = 12821$, a value much larger than the neutral value for the instability of the conducting quiescent state, which is $Ra_{c1} = 2424$ for $m = 1$ (figure 2). The thermal energy balance (figure 7) shows that the strong stabilization is due to I_{T2}, which is the only stabilizing quantity besides the heat diffusion rate D_T. It is a measure of the vertical heat transfer process related to the convective deformation Θ of the conducting temperature profile Θ_{cond}.

Since the classical buoyant instability mechanism delays the second thermal instability due to the stabilizing influence of the primary temperature field, this instability cannot be observed for low Prandtl numbers. For low Pr the primary axisymmetric flow becomes unstable at much lower Rayleigh numbers due to an inertial instability, which is absent for high Pr.

Opposite to the case $Pr = 0.02$, no change in the mechanism of the instability occurs when Γ is increased. Thermal and kinetic energy balances show a similar behaviour throughout the investigated Γ-interval. For $\Gamma = 1.46$, the instability becomes oscillatory with $m = 3$ being the critical mode. Still, I_{T3} is the most destabilizing contribution to the thermal energy balance; the above described mechanism for $m = 1$ is still valid. However, there must be an additional effect that is responsible for the onset of oscillations.

Figures 8 and 9 show the temperature fields at $\varphi = 0$ of two typical critical modes, a stationary ($m = 1$) and an oscillatory ($m = 3$) one. A cold region can be identified at $r \approx 0.8, z = -0.15$ for $m = 3$ (figure 9), that is not present for $m = 1$. It is generated by a radial outward disturbance flow transporting cold fluid from the basic-state temperature distribution (figure 10). The horizontal disturbance temperature distribution (figure 9) in turn is unstable and tends to create a radial inward flow for $z < 0$, which, however, would be opposite to the present disturbance velocity field. This frustration is resolved by a clockwise azimuthal rotation of the

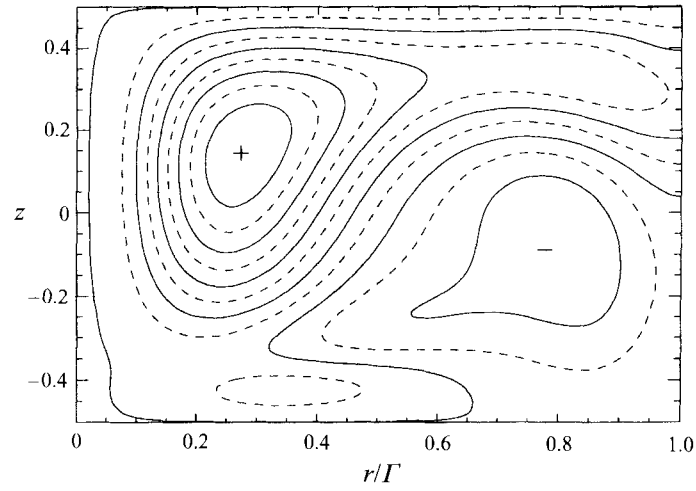

FIGURE 9. Temperature field of the critical mode at $\varphi = 0$ for $\Gamma = 1.47$, $Pr = 1$, $Ra_{c2} = 24928$, $m = 3$. The dimensionless oscillation frequency is $\omega_{c2} = 42.5$.

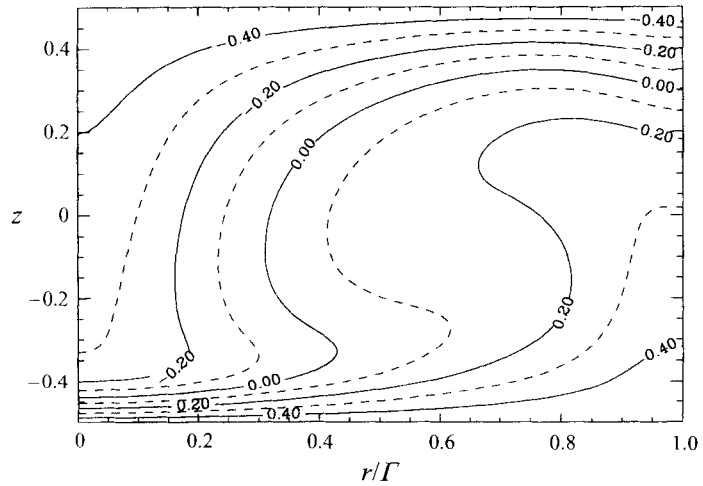

FIGURE 10. Temperature field of the axisymmetric basic state $(\Theta + \Theta_{cond})$ for $\Gamma = 1.47$, $Pr = 1$, $Ra = Ra_{c2} = 24928$.

critical mode. Owing to this rotation, an azimuthal phase shift of the temperature minima arises relative to the flows that generate them. The phase shift can be seen in figure 11 showing a horizontal cross-section at $z = -0.3$ viewed from above. The maximum radial outward flow occurs at a different azimuthal angle (full line in figure 11*b*) than that of the corresponding cold region (dotted line); the frustration is resolved. The same arguments (with different signs) hold for the temperature maxima generated by radial inward flow. Oscillations are absent for $m = 1$, because the critical mode involves no significant radial outward flow that could generate a cold spot. The structure of the neutral mode is qualitatively the same along both oscillatory instability curves, $m = 3$ and $m = 4$.

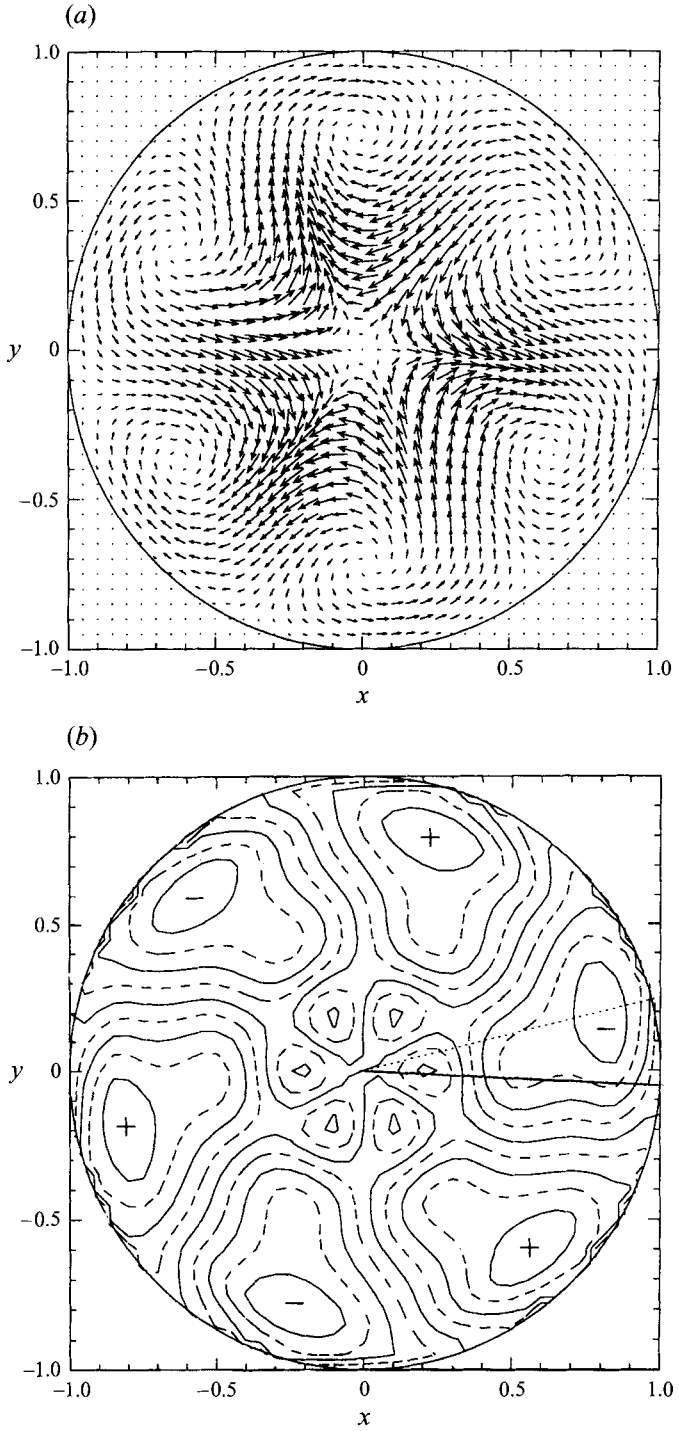

FIGURE 11. Disturbance flow (*a*) and temperature (*b*) fields of the critical mode in an axial cross-section at $z = -0.3$ for $\Gamma = 1.47$, $Pr = 1$, $Ra_{c2} = 24928$, $m = 3$. The full line in (*b*) indicates the azimuthal position of maximum radial outward flow, the dotted line indicates that of the temperature minimum.

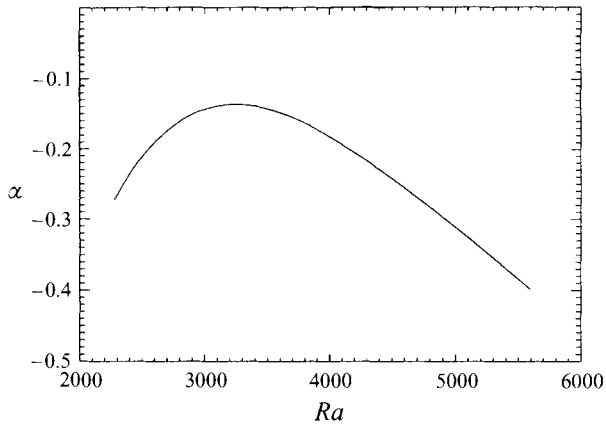

FIGURE 12. Growth rate α of the mode $m = 2$ as a function of Ra for $Pr = 6.7$, $\Gamma = 1$.

4.2.3. $Pr = 6.7$

For $\Gamma = 1$ and $Pr = 6.7$, Hardin & Sani (1993) within their weakly nonlinear approach found a stationary bifurcation to an $m = 2$ mode at $Ra_{c2} = 2850$. We find $m = 2$ to be linearly stable for these parameters. However, the growth rate of the $m = 2$ mode has a negative maximum at $Ra = 3216$ (figure 12). This behaviour is qualitatively identical to that for $Pr = 1$ where the maximum takes a positive value rendering $m = 2$ unstable in a small Rayleigh number interval. If the instability is supercritical for these parameters a weakly nonlinear three-dimensional state may result. For $Pr = 6.7$, we find that the basic flow becomes unstable first to a mode with symmetry $m = 1$ at $Ra_{c2} = 10134$ in qualitative agreement with the experimental result of Müller *et al.* (1984) ($Ra_{c2} \approx 10 Ra_{c1} = 22600$).

5. Concluding remarks

The instability of axisymmetric Rayleigh–Bénard convection in a cylindrical layer depends qualitatively on the Prandtl number. For large Prandtl numbers (here $Pr = 1$ and $Pr = 6.7$) the two-dimensional flow becomes unstable due to the classical thermal instability mechanism. The temperature field of the axisymmetric base state acts to stabilize non-axisymmetric disturbances. Thus the two-dimensional flow remains linearly stable up to large Rayleigh numbers, e.g. $Ra_{c2}(\Gamma = 1.4, Pr = 1, m = 1) = 22493$. At these high Rayleigh numbers, the basic two-dimensional flow of low Prandtl number fluids involves high-inertia velocity fields, which become unstable prior to thermal instability. The mechanism is inertial in character. The maximum Rayleigh number for which the flow is two-dimensional is approximately $Ra_{c2}(\Gamma = 1.3, Pr = 0.02, m = 2) = 3506$. Thus there must be some transition range at intermediate Prandtl numbers within which the instability mechanism changes from inertial to thermal.

The present results for $Pr = 0.02$ are in good agreement with previous numerical work (Neumann 1990; Hardin & Sani 1993). For $Pr = 6.7$ and $\Gamma = 1$, however, we have shown that the axisymmetric flow is linearly stable with respect to $m = 2$ modes. This supports the recent numerical simulation of Wagner *et al.* (1994) and it is in agreement with the experiments by Müller *et al.* (1984). We conclude that the previous calculations of Müller *et al.* (1984), Neumann (1990) and Hardin & Sani (1993), who either found a nonlinear convective state with $m = 2$ at $Ra \approx 2800$ or a

supercritical bifurcation to an $m = 2$ mode, are in error. The present linear stability calculation cannot preclude the existence of a finite-amplitude $m = 2$ mode. However, since Wagner *et al.* (1994) proved the exponential decay of an $m = 2$ disturbance from a finite initial amplitude for $Ra = 2800$, there is evidence for the absence of such a state. Given the growth rate dependence of the $m = 2$ mode on Ra (figure 12) together with the stability diagram for $Pr = 1$ (figure 6), we anticipate that the linear stability diagram for $Pr = 6.7$ is topologically similar to that for $Pr = 1$. Thus the reason for the numerical difficulties encountered by some previous investigations for $\Gamma = 1$ becomes clear. On increasing Ra for the constant aspect ratio $\Gamma = 1$ the linearly unstable range for $m = 2$ is just missed. For a slightly smaller aspect ratio the basic flow should become unstable to an $m = 2$ mode, although the amplitude can be expected to remain small.

The authors are very grateful to M. Prange for running the numerical program, for collecting the data and for stimulating discussions. We are also indebted to V. M. Shevtsova for providing the program for the energy balance computations. This work was supported by DFG under grant number Ku896/2.

REFERENCES

BOHM, J., LÜDGE, A. & SCHRÖDER, W. 1994 Crystal growth by floating zone melting. In *Handbook of Crystal Growth Vol. 2a : Bulk Crystal Growth* (ed. D. T. J. Hurle) p. 213. Elsevier.

BUELL, J. C. & CATTON, I. 1983 The effect of wall conduction on the stability of a fluid in a right circular cylinder heated from below. *Trans. ASME J. Heat Transfer* **105**, 255.

BUSSE, F. H. 1978 Non-linear properties of thermal convection. *Rep. Prog. Phys.* **41**, 1929.

CHARLSON, G. S. & SANI, R. L. 1970 Thermoconvective instability in a bounded cylindrical fluid layer. *Intl J. Heat Mass Transfer* **13**, 1479.

CHARLSON, G. S. & SANI, R. L. 1971 On thermoconvective instability in a bounded cylindrical fluid layer. *Intl J. Heat Mass Transfer* **14**, 2157.

CHARLSON, G. S. & SANI, R. L. 1975 Finite amplitude axisymmetric thermoconvective flows in a bounded cylindrical layer of fluid. *J. Fluid Mech.* **71**, 209.

CHEN, Y. Y. 1992*a* Boundary conditions and linear analysis of finite-cell Rayleigh–Bénard convection. *J. Fluid Mech.* **241**, 549.

CHEN, Y. Y. 1992*b* Finite-size effects on linear stability of pure-fluid convection. *Phys. Rev.* A **45**, 3727.

CRESPO DEL ARCO, E. & BONTOUX, P. 1989 Numerical simulation and analysis of axisymmetric convection in a vertical cylinder: An effect of Prandtl number. *Phys. Fluids* A **1**, 1348.

HARDIN, G. R. & SANI, R. L. 1993 Buoyancy-driven instability in a vertical cylinder: Binary fluids with Soret effect. Part 2: Weakly non-linear solutions. *Intl J. Numer. Meth. Fluids* **17**, 755.

HARDIN, G. R., SANI, R. L., HENRY, D. & ROUX, B. 1990 Buoyancy-driven instability in a vertical cylinder: Binary fluids with Soret effect. Part 1: General theory and stationary stability results. *Intl J. Numer. Meth. Fluids* **10**, 79.

KOSCHMIEDER, E. L. 1993 *Bénard Cells and Taylor Vortices.* Cambridge University Press.

LIANG, S. F., VIDAL, A. & ACRIVOS, A. 1969 Buoyancy-driven convection in cylindrical geometries. *J. Fluid Mech.* **36**, 239.

MÜLLER, G., NEUMANN, G. & WEBER, W. 1984 Natural convection in vertical Bridgeman configurations. *J. Cryst. Growth* **70**, 78.

NEUMANN, G. 1986 Berechnung der thermischen Auftriebskonvektion in Modellsystemen zur Kristallzüchtung. Dissertation, Technische Fakultät der Universität Erlangen-Nürnberg.

NEUMANN, G. 1990 Three-dimensional numerical simulation of buoyancy-driven convection in vertical cylinders heated from below. *J. Fluid Mech.* **214**, 559.

ROSENBLAT, S. 1982 Thermal convection in a vertical circular cylinder. *J. Fluid Mech.* **122**, 395.

STORK, K. & MÜLLER, U. 1975 Convection in boxes: An experimental investigation in vertical cylinders and annuli. *J. Fluid Mech.* **71**, 231.

WAGNER, C., FRIEDRICH, R. & NARAYANAN, R. 1994 Comments on the numerical investigation of Rayleigh and Marangoni convection in a vertical cylinder. *Phys. Fluids* **6**, 1425.

WANSCHURA, M., SHEVTSOVA, V. M., KUHLMANN, H. C. & RATH, H. J. 1995 Convective instability mechanisms in thermocapillary liquid bridges. *Phys. Fluids* **7**, 912.